Available online at www.sciencedirect.com
ScienceDirect
Journal of the European Ceramic Society 30 (2010) 1691–1698
www.elsevier.com/locate/jeurceramsoc

Yttria stabilized zirconia synthesis in supercritical CO_2: Understanding of particle formation mechanisms in CO_2/co-solvent systems

Audrey Hertz [a,*], Yves-Marie Corre [a], Stephane Sarrade [b], Christian Guizard [c], Anne Julbe [d], Jean-Christophe Ruiz [a], Bruno Fournel [e]

[a] CEA Marcoule DEN/DTCD/SPDE/LFSM, BP 17171, 30207 Bagnols sur Cèze, France
[b] CEA Marcoule DEN/DTCD/SPDE, BP 17171, 30207 Bagnols sur Cèze, France
[c] Laboratoire de Synthèse et Fonctionnalisation des Céramiques, UMR 3080 CNRS, SAINT-GOBAIN C.R.E.E., 550 Avenue Alphonse Jauffret, BP 224, 84306 Cavaillon, France
[d] Institut Européen des Membranes, UMR 5635 CNRS-UMII-ENSCM, UM2-CC047, Place Eugène Bataillon, 34095 Montpellier Cedex 5, France
[e] CEA Marcoule DEN/DTCD, BP 17171, 30207 Bagnols sur Cèze, France

Received 24 September 2009; received in revised form 17 December 2009; accepted 10 January 2010

Abstract

The increasing interest of supercritical (SC) fluids for inorganic materials synthesis recently stimulated the development of innovative synthesis processes and strategies. The supercritical CO_2 aided sol–gel process, developed for preparing various ceramic oxide powders with attractive applications in cosmetics, chromatography, catalysis or solid oxide fuel cells, usually suffer from both reproducibility problems and poor knowledge of the key parameters defining the final powder characteristics. In the present work a specific effort has been put on the understanding of reaction mechanisms and process parameters like co-solvent polarity and ageing time of the starting solution, which appeared to play a crucial role for the control of powder characteristics. Two different reaction mechanisms have been proposed to explain the formation of tetragonal yttria-doped zirconia powders by a batch process in either CO_2/pentane or CO_2/isopropanol mixtures. The first mechanism corresponds to a CO_2 anti-solvent precipitation process while the other one is based on a condensation reaction as in the conventional sol–gel process. This improved understanding in particle formation allows better control of powder characteristics and reproducibility.

Keywords: Supercritical CO_2; Sol–gel processes; Y-ZrO_2; Powder-chemical preparation; Porosity

1. Introduction

Supercritical fluids exhibit a large range of unusual properties that can be exploited for preparing original materials differing from those derived from classical methods. Supercritical water[1,2], alcohols[3–6] or carbon dioxide[7–11] have been namely considered for the preparation of various ceramic oxides. The interest of the supercritical carbon dioxide (SC-CO_2) aided sol–gel process has been specifically demonstrated for the synthesis of ceramic materials as SiO_2 fibers or powders,[12] TiO_2 powders,[8] and various nanopowders of ion-conducting ceramics.[7,9] The ceramic powders synthesized by this method do not need any filtration or drying step, and their crystallization temperature is generally much lower compared to usual processes (e.g. conventional sol–gel process).

These powders afford new technological developments based on the specific properties of nanophase ceramics. For example, worldwide current research efforts in solid oxide fuel cells (SOFCs) are focused on lowering the operating temperature down to 1000 K (IT-SOFC) and among other parameters, on the control of the microstructure and composition of ceramic electrolytes. In previous works, we have shown the interest of SC-CO_2 derived gadolinium-doped ceria (CGO) and yttria-doped zirconia (tetragonal 3Y-TZP) powders for this application.[7] The oxygen conductivity of sintered pellets derived from CGO powders prepared in SC-CO_2 was measured by impedance spectroscopy and was evidenced to be higher than the one measured for doped ceria prepared by other methods

* Corresponding author.
E-mail address: audrey.hertz@cea.fr (A. Hertz).

0955-2219/$ – see front matter © 2010 Elsevier Ltd. All rights reserved.
doi:10.1016/j.jeurceramsoc.2010.01.021

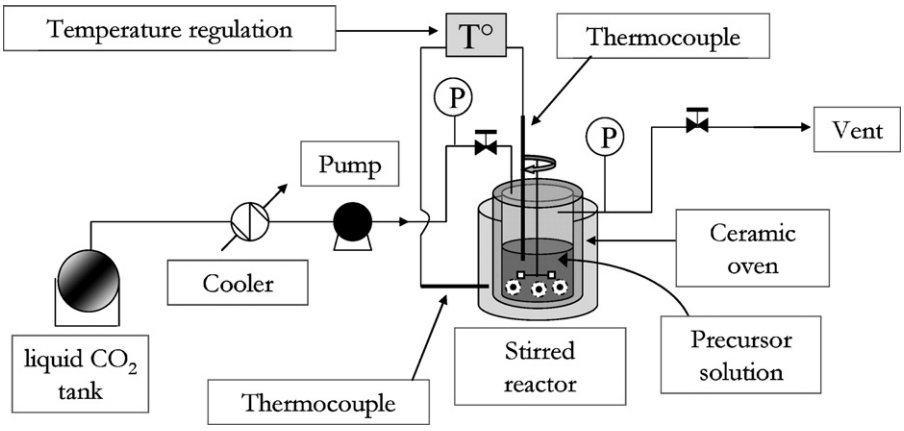

Fig. 1. Experimental set-up used for the synthesis of 3Y-TZP powders by the batch process.

like conventional sol–gel process or hydrothermal synthesis.[9] On the other hand processing of 3Y-TZP for producing a dense electrolyte was hardly achieved due to fluctuating powder characteristics. Moreover, the tetragonal to monoclinic phase transition (t-m) occurring during the sintering process led to the degradation of conductivity properties. Works from the literature showed that structural parameters such as mean grain size, grain size distribution, porosity[13] and yttrium distribution[14] are supposed to control this phase transition. So a better understanding of both the involved reaction mechanisms and their influence on the structural parameters is of great importance to control the powder characteristics and their sintering behavior.

In this work, we focused on the dissolution capacity of the supercritical solvent and co-solvent used as reaction media and more precisely on the behavior of the CO_2/co-solvent binary mixture. A decisive stage responsible for reproducibility problems in this one step batch process occurs when temperature and pressure are raised in order to obtain a crystalline powder through the drastic anti-solvent effect of SC-CO_2. Specific attention has been paid to understand the different steps involved during the formation of 3Y-TZP (tetragonal zirconia polycrystal doped with 3 mol% yttria) particles. The role of key parameters such as co-solvent type and precursor solution ageing time has been also emphasized.

2. Experimental

2.1. Chemicals

Precursors used for 3Y-TZP powder synthesis were zirconium hydroxyacetate ($Zr(acetate)_x(OH)_y,zH_2O$ $(x+y=4)$) and yttrium acetate ($Y(acetate)_3,xH_2O$). The acetate precursors were mixed in either pentane (99%, PROLABO) or 2-propanol (+99%, ALDRICH). Nitric acid (65%, HNO_3-FLUKA) was used as a dissolution additive, yielding clear, homogeneous and stable solutions.

2.2. Synthesis reactor

A schematic representation of the experimental set-up used for powder batch synthesis in SC-CO_2 medium is shown in Fig. 1. It consists in a stainless steel autoclave, mechanically stirred and working in a discontinuous mode. The internal volume of the reactor is 0.5 l, and the maximal operating conditions are 623 K and 30 MPa.

For each experiment, the reactor was operated according to the following procedure: after introducing a solution of reactants, the reactor was closed and CO_2 was injected at room temperature up to 4–5 MPa, depending on the required final pressure and temperature. Then stirring and heating (external electric heater) were started. The increase of temperature induces an increase of pressure following an isodensity curve. Final temperature and pressure were maintained from several minutes to few hours (reaction time) in order to allow the formation of the crystalline ceramic powder. Finally, temperature was decreased and CO_2 was vented. Finally, the reactor was opened and reaction products were collected.

2.3. 3Y-TZP synthesis

The synthesis of 3Y-TZP (∼3 mol% Y_2O_3) powders can be schematically described as a SC-CO_2 aided sol–gel process. First the zirconium and yttrium acetates (7.5 and 1 g, respectively) were mixed in either 50 ml of pentane or 50 ml of 2-propanol (co-solvent) and 5 ml of nitric acid was added as dissolution-aiding agent. The effect of solution ageing time (maturation) before supercritical treatment was studied in the range 0–1200 h.

Then, reaction was carried out in SC-CO_2 during 1 h at 30 MPa and 523 K for pentane solutions (88 mol% CO_2) or 623 K for 2-propanol solutions (78 mol% CO_2). The synthesis parameters (temperature, pressure, reaction time) were selected in order to obtain a crystalline powder with high specific surface area. After reaction completion (1 h), CO_2 was vented and temperature slowly decreased; the reactor was opened and ceramic oxide particles were recovered in ambient conditions.

2.4. Characterization methods

Crystalline phases were determined by X-ray diffraction (Brucker D800) on powders and crystallite sizes were determined by the Scherrer formula from (1 0 1) diffraction lines for

Table 1
Structural and textural characteristics of the 3Y-TZP powders prepared with the discontinuous process, from pentane solutions with different ageing times. Synthesis was performed at 250 °C, 30 MPa for 1 h.

Ageing time (h)	Monoclinic phase (%)	Mean crystallite size (nm)	Mean particle sizes (nm)	Specific surface area (m^2/g)
No	57	22	65	–
No	64	15	–	70
0.33	0	23	49	32
0.33	0	/	65	30
0.33	<5	22	50 and 190	49
3	0	24	–	64
17	0	26	50 and 210	38
41	0	29	50 and 200	12
65	0	25	90 and 170	105
92	0	27	140	49
120	0	29	90	–

the tetragonal structure, (1 1 1) for the cubic one and ($\bar{1}$ 1 1) for the monoclinic one. The fractions of monoclinic phase (f_M) in doped zirconia powders were determined from intensities (I) of monoclinic (M) and tetragonal (T) lines according to the following equations:

$$f_M = \frac{1.311 \times X_M}{1 + 0.311 \times X_M} \quad \text{with}$$

$$X_M = \frac{I_M(\bar{1}\,1\,1) + I_M(1\,1\,1)}{I_M(\bar{1}\,1\,1) + I_M(1\,1\,1) + I_T(1\,0\,1)}$$

The morphology and particle sizes of the produced powders were studied using scanning electron microscopy (FESEM-Hitachi S4500). Powder specific surface areas and average pore sizes were determined, after 24 h outgassing at 523 K, by applying the BET and BJH equations to the adsorption curve of the N_2 adsorption–desorption isotherms (Micromeritics-ASAP 2010).

2.5. Transparent cell

A transparent reactor made of sapphire monocrystal has been used for visual observations during the synthesis process, in order to evaluate the behavior of the reactive mixture during pressurisation with CO_2 and heating. The cell volume is about 36 ml and the apparatus can withstand maximal pressure and temperature conditions of 50 MPa and 573 K. No stirring was applied and heating was achieved by placing the cell inside a drying oven.

3. Results

3.1. Synthesis from precursors in pentane solutions

Results reported in Table 1 show that an increased ageing time only leads to a slight increase in mean crystallite sizes (from 15 to 30 nm) for the powders derived from pentane solutions. More interesting is the influence of this parameter on the formed crystalline phases: only 20 min sol ageing are enough for a quasi-complete stabilization of the tetragonal phase.

Fig. 2 shows the effect of pentane solution ageing time on the mean particle size. Short ageing times (shorter than 20 min) mainly yield small particles (sizes in the range 50–65 nm). Long ageing times (longer than 90 h) generate bigger particles (size in the range 90–140 nm). Intermediate ageing times generally yield a double size distribution, with the smallest one centered on 50 nm and the biggest around 200 nm. Finally, no obvious tendency was observed concerning the influence of ageing time on the specific surface area of powders derived from pentane solutions.

3.2. Synthesis from precursors in 2-propanol solutions

When 2-propanol was used as co-solvent, ageing time of the precursor solution was found to influence neither the tetragonal to monoclinic phase transition, nor the particle size (Table 2). On the contrary, quite reproducible crystallite sizes and specific surface areas were obtained whatever the ageing time.

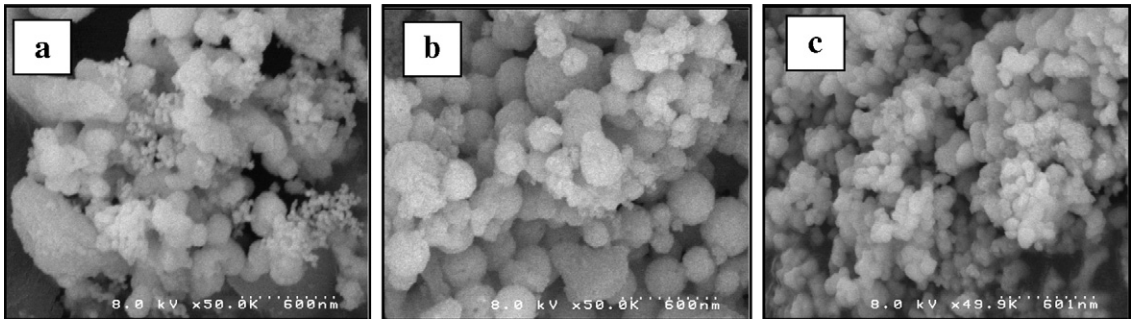

Fig. 2. FESEM micrographs showing the morphology of 3Y-TZP particles synthesized from pentane solution after different ageing times: (a) 17 h, (b) 41 h and (c) 120 h.

Table 2
Structural and textural characteristics of the 3Y-TZP powders prepared with the discontinuous process, from 2-propanol solutions with different ageing times. Synthesis was performed at 350 °C, 30 MPa for 1 h.

Ageing time (h)	Monoclinic phase (%)	Crystallite size (nm)	Mean particle size (nm)	Specific surface area (m^2/g)
3	0	6	–	186
17	46	6.5	678	218
17	35	6.5	472	143
41	0	5.5	–	205
65	16	5.5	1064	–
65	14	6.5	560	193
160	10	6.5	–	–
720	55	7	383	215
1200	24	7	760	–

Fig. 3 shows particle sizes and morphology for different solution ageing times. Spherical particles are principally obtained but, either sintered aggregates, or a bimodal particle size distribution are observed. Finally, compared to pentane, bigger particle sizes and higher specific surface areas (almost 200 m^2/g) were obtained with 2-propanol as co-solvent.

As shown in Table 3, these comparative experiments with a non-polar (pentane) or a polar (2-propanol) co-solvent revealed very different behaviors, and lead to totally different powder characteristics.

4. Discussion on parameters influencing 3Y-TZP powder characteristics

4.1. Tetragonal phase stabilization and crystallite sizes

For pentane solutions, a sizeable effect of ageing time was noticed, especially related to the tetragonal phase stabilization and crystallite size. This behavior was not observed for 2-propanol solutions. This is likely to be linked with precursor solution characteristics.

In fact, a gelation phenomena was observed with pentane and the time needed for gel formation corresponds to the tetragonal phase stabilization (20 min ageing time) during the supercritical treatment. Stabilization of the tetragonal phase could then be explained in this case by the reaction of ceramic precursors at the molecular level during gel formation. The solution prepared with 2-propanol never formed a gel and obviously the tetragonal phase does not form by reaction of the precursors at this stage of the process. In conclusion, the dispersion of yttrium in the zirconia structure occurs at the sol stage before the supercritical treatment for pentane solutions, while it is probably thermally activated during the supercritical treatment for 2-propanol solutions. Consequently, the tetragonal zirconia stabilization is improved using pentane solution thanks to a more homogenized and controlled yttria distribution inside the zirconia structure.

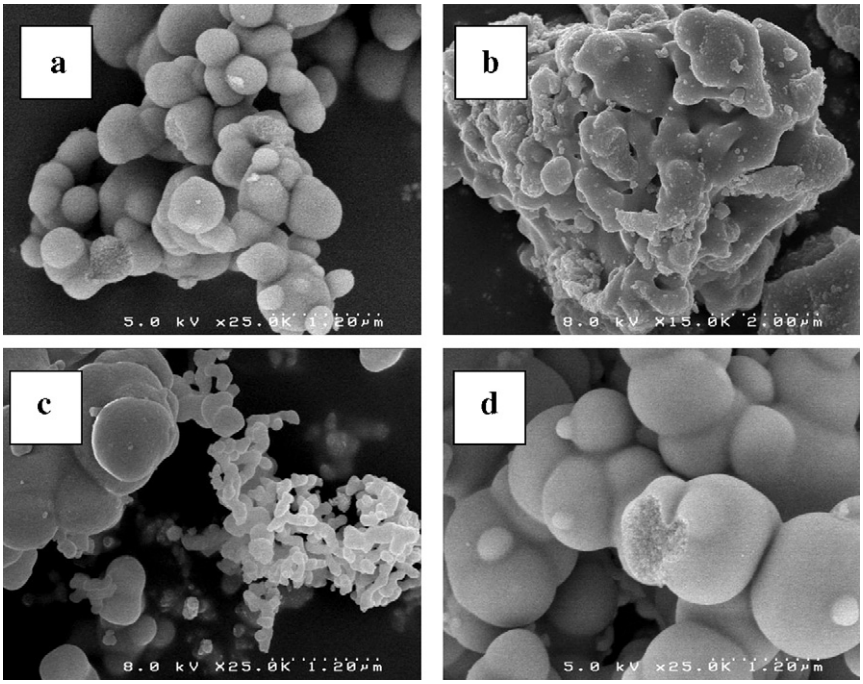

Fig. 3. FESEM micrographs showing the morphology of 3Y-TZP particles synthesized from 2-propanol solution after different ageing times: (a) 17 h, (b) 41 h, (c) 65 h and (d) 160 h.

Table 3
Main characteristics of the 3Y-TZP depending on the co-solvent.

	Pentane	2-Propanol
Characteristic of the mother solution	Gelation after 20 min ageing	Transparent solution whatever the ageing time
Crystallite sizes (XRD)	From 15 to 30 nm	From 5 to 7 nm
Particle sizes (SEM)	From 50 to 250 nm	From 200 nm to 3 μm
Specific surface area (S_{BET})	From 10 to 100 m^2/g	From 140 to 220 m^2/g
Morphology (FESEM)	One or two populations of spherical particles	One or two populations of spherical particles—sometimes sintered aggregates
Influence of ageing time	Tetragonal phase stabilization Slight effect on crystallite sizes Effect on particle size distribution	No clear tendency was evidenced

In addition, gel formation in pentane solution might also be responsible for the increasing crystallite sizes with ageing time. Indeed, isopropanol solutions seems stable and crystallites remain small (5–7 nm) whatever the ageing time, while crystallites are bigger (15–30 nm) and ageing time dependant when pentane is employed. Cluster growth by condensation reaction explains both the increasing crystallite sizes and gel formation in pentane solution.

4.2. Textural and structural characteristics

The SC-CO_2 assisted sol–gel process resulted in 3Y-TZP powders with high specific surface area (10–220 m^2/g), depending especially on the used co-solvent. It has been shown that these specific surface area values (S in m^2/g) were directly correlated with crystallite sizes following the equation $S = 3/(r \times \rho)$, with ρ the theoretical density (6.10 g/cm^3) and r the particle/crystallite radius (μm). N_2 adsorption/desorption method also evidenced the presence of bimodal pore size distribution in 3Y-TZP powders prepared in supercritical CO_2. Intra-particle micro/mesopores smaller than 4 nm in diameter and inter-particle macropores of about 30–50 nm in diameter have been observed. These pores results from aggregation of crystallites and particles, respectively. Indeed, SEM and TEM observations in Fig. 4 illustrate the typical multi-scale structure of the particles derived from this batch synthesis process: nanocrystallites are aggregated in spherical particles.

The size of spherical particles also depends on the type of co-solvent selected for preparing the initial precursor solution. For synthesis realized with pentane solutions ageing time seems to control the particle size (Tables 1 and 3). Two particle size populations have been evidenced: the first one in the range of 30–100 nm and the second one in the range of 100–200 nm. The small particles in population 1 derive from clusters formed in the gel phase (previously described). The increase of crystallite sizes with ageing time could explain the increase in particle size. Agglomeration of small particles during maturation phase might result in the second particle population. After 40 h ageing time, particle sizes of both populations tend to homogenize through progressive reorganization of agglomerates or/and by Oswald

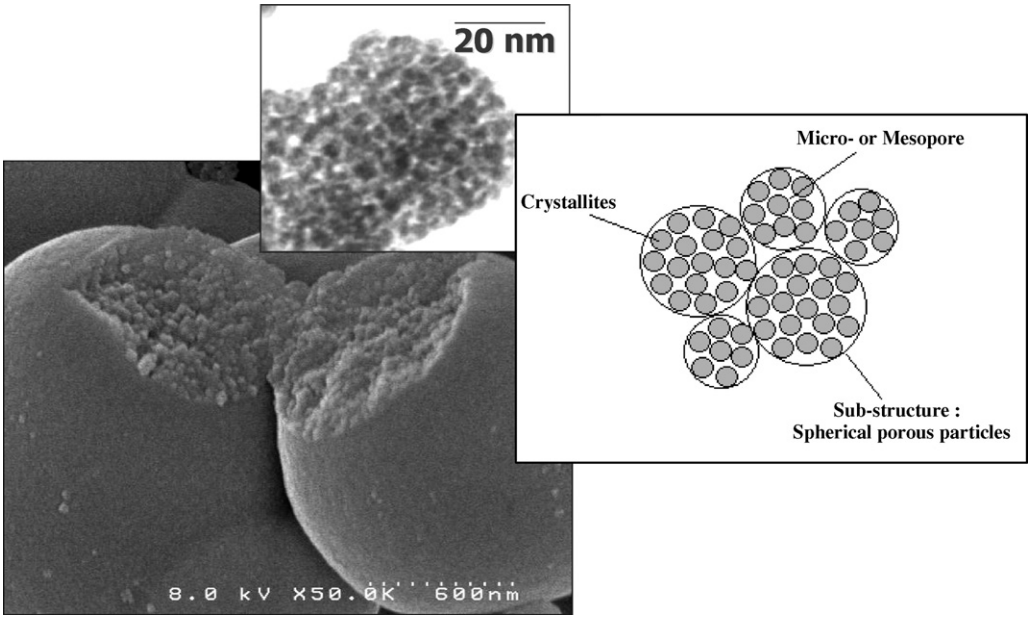

Fig. 4. FESEM and TEM micrographs showing the multi-scale powder microstructure. Aggregated nanocrystallites form porous nano- or microparticles which are also able to form aggregates.

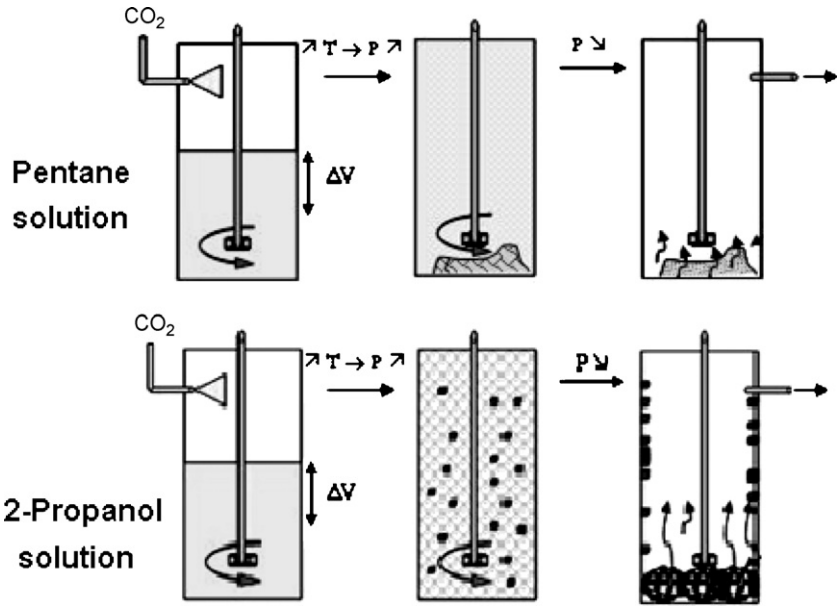

Fig. 5. Schematic representation of reactive solution behavior during 3Y-TZP supercritical CO_2 synthesis, based on visual observations (transparent cell) and depending on the co-solvent.

ripening mechanism. After 90 h ageing time only one particle size population remains at an intermediate size. For 2-propanol solutions, no gel formation is observed and ageing time does not influence particle size and morphology (Tables 2 and 3). In this case, the mechanism for particle formation is initiated in pressurized CO_2.

4.3. Key parameters controlling 3Y-TZP powder characteristics

The co-solvent polarity is an influential factor for the final powder characteristics. A judicious selection of the co-solvent for sol preparation allows controlling both powder crystallite sizes and specific surface areas. The use of polar co-solvent (2-propanol in this study) instead of non-polar co-solvent (pentane) favors the formation of valuable powders with high specific surface area and small crystallite sizes.

On the contrary, with this discontinuous process, particle size and crystalline structure can be controlled only by using the non-polar co-solvent (pentane in this study). In this case, the tetragonal phase is stabilized and particle size distribution is controlled by choosing the appropriate solution ageing time.

5. Discussion about particle formation mechanisms

5.1. Visual observations and reactive solution behavior

Observation of the co-solvent/CO_2 mixtures in a transparent cell and comparison between pentane and 2-propanol helped better understanding the involved reaction mechanisms (Fig. 5).

For the pentane solution, gel formation can occur rapidly (20 min) and condensation reaction can be observed before reactor pressurisation with CO_2. After CO_2 introduction into the reactor and during the heating stage, total miscibility between pentane and CO_2 was observed at low temperature ($T_c \sim 323$ K). Then, particle precipitation rapidly occurred due to the SC-CO_2 anti-solvent and sursaturation effects.

For the 2-propanol solution, gelation is not observed. After CO_2 pressurisation in the reactor and during the heating stage, total miscibility of 2-propanol and CO_2 occurred at higher temperature ($T_c \sim 373$ K) than with pentane. A biphasic media (liquid/gas) can be observed inside the reactor. Thus, nucleation and growth due to reactant condensation could start in the liquid phase before the CO_2 anti-solvent effect yields particle formation.

In fact, these observations reveal that pressurization and heating stages, leading to final synthesis conditions, are key parameters for controlling particle formation mechanisms and need to be studied in more details.

5.2. Binary phase diagram study

In order to better understand the effect of the reaction media on powder characteristics, a detailed study on CO_2/co-solvent behavior was carried out. Phase diagrams have been built for the two CO_2/co-solvent mixtures (Figs. 6 and 7), i.e. (i) 0.88 mol fraction of CO_2 for the CO_2/pentane mixture ($T_c \sim 328$ K and $P_c \sim 8$ MPa) and (ii) 0.78 mol fraction of CO_2 for the CO_2/2-propanol mixture ($T_c \sim 378$ K and $P_c \sim 13$ MPa) using literature data.[15–19] Literature data for mixture critical temperatures are close to the experimental values observed with the transparent cell.

Pressurization/heating curves (black dashed curve in Figs. 6 and 7) have been reported onto the phase diagrams. These curves have been obtained during the reactor heating stage, by measuring the pressure for each temperature, from room temperature to final operating temperature. For isopropanol/CO_2 mixtures, initial reactor pressure was fixed at 5.3 MPa (at room temperature) in order to reach the final temperature of 623 K and pressure of 30 MPa. For pentane/CO_2 mixtures, initial reactor

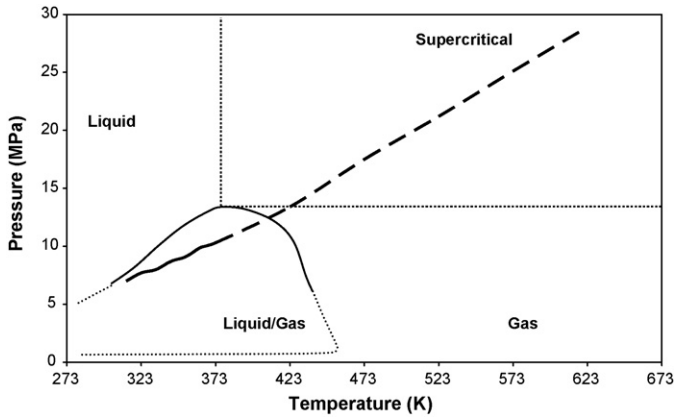

Fig. 6. CO_2/2-propanol phase diagram for 0.78 molar fraction of CO_2 (temperature/pressure representation). Final temperature = 623 K, final pressure = 30 MPa.

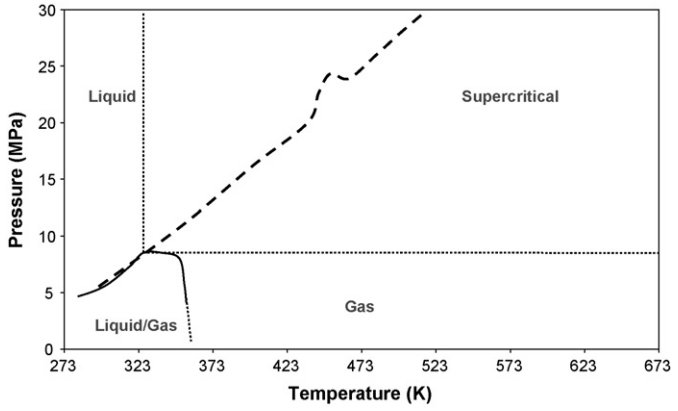

Fig. 7. CO_2/pentane phase diagram for 0.88 molar fraction of CO_2 (temperature/pressure representation). Final temperature = 623 K, final pressure = 30 MPa.

pressure was fixed at 5 MPa (at room temperature) in order to reach the final temperature of 523 K and pressure of 30 MPa.

First, a specific artefact at around 450 K corresponding to an exothermal reaction can be noticed using pentane co-solvent. An intermediate nitrate compound resulting from the reaction between nitric acid and acetate precursors is formed, which decomposes to oxides at 450 K. This compound does not form when using 2-propanol co-solvent.

Then, two differences can be noticed when comparing the location of phase areas (liquid, gas, liquid/gas and supercritical) vs. temperature for the two CO_2/co-solvent mixtures. The first one concerns the delay (t_s) before entering the supercritical area: 5 min with pentane co-solvent and 25 min with 2-propanol, with the same heating rate in both cases (300 K/h). Heating duration under supercritical conditions (before reaching the operating temperature and pressure value) is equivalent for both compositions and last 20 min. The second difference is related to the type of phase which is met when temperature is increased: mainly liquid for CO_2/pentane and liquid/gas for CO_2/2-propanol.

Particle formation mechanisms related to anti-solvent phenomenon and liquid phase condensation (mentioned before) fit these phase diagram descriptions.

5.3. Possible mechanisms occurring during 3Y-TZP powder synthesis

SEM/TEM observations and phase diagram study bring about the consideration of two different mechanisms for particle formation. In addition to cluster/particle formations during solution maturation (before supercritical treatment), two competitive mechanisms take place within the reactor, under pressurized CO_2 environment. The short delay (t_s = 5 min), before entering the homogeneous supercritical pentane/CO_2 medium, is compatible with the hypothesis of anti-solvent precipitation and gel-drying mechanisms. Consequently, particle formation occur through both condensation reactions in air (in the Becker), and CO_2 anti-solvent effects (in the reactor). For pentane/CO_2 reaction media, two successive mechanisms controlling crystalline structure and particle size could be attributed to the effects of both maturation and supercritical treatment. The first mechanism takes place during ageing of the starting solution in which condensation of yttrium and zirconium cations give rise to cluster growth and gel formation. The second mechanism occurs during the treatment in pressurized CO_2, with first the dispersion of the gel phase in the CO_2/pentane mixture and then the growth of crystalline particles by a combined effect of temperature and anti-solvent process.

For 2-propanol/CO_2 mixture, the slow transition to reach supercritical conditions (t_s = 25 min) confirm the hypothesis of condensation within the liquid phase. Reaction between hydrated cations followed by nucleation and particle growth mainly occurs into the reactor during the pressurized CO_2 treatment. In fact, hydrolysis of yttrium and zirconium salts yields hydrated cations in 2-propanol, but condensation reactions are limited by the acidic pH of the starting sol. In this case, particle formation rather results from a complete process in CO_2 media (in the reactor) involving precursor reaction, seed formation and particle growth. Particles formation by condensation reaction in liquid phase is obtained by cluster growth and particle precipitation when clusters reach a critical size. The progressive increase in CO_2 concentration within the liquid phase and the evaporation of isopropanol into the gas phase before reaching supercritical conditions (t_s = 25 min) could lead to several particle precipitations by anti-solvent effect, explaining the polydispersity of the 3Y-TZP particle size distribution.

Consequently, the "delay" before entering the supercritical area appears as a very decisive parameter for controlling powder characteristics and the influence of mass transfer on particle and crystallite formation is noticeable. The different crystallite sizes obtained when using pentane or 2-propanol might be related to the difference in mass transfer between the co-solvent and the CO_2 phases, leading to different supersaturation rates.[20] Indeed, in the liquid/gas biphasic area, droplets can form due to stirring. Mass transfer between the CO_2-rich and the co-solvent-rich phases occurs and its kinetic depends on the co-solvent properties. Moreover, co-solvent/CO_2 mixture properties, especially precursor diffusivity, might strongly depend on the co-solvent properties, thus affecting reaction kinetics. Therefore, mass transfer can be modulated by selecting the appropriate co-solvent, and reaction kinetics might be monitored carefully.

6. Conclusions

Ceramic processing in SC-CO_2 is a very promising technique for creating nanocrystalline and homogeneous mixed oxide ceramic powders from salts or metal-organic compounds. As shown for yttria stabilized zirconia, combining the sol–gel method with the anti-solvent property of SC-CO_2 leads to a very versatile process well adapted to the production of crystalline powders with high specific surface area. Yttria-doped zirconia powders, stabilized in tetragonal phase, were successfully prepared with this method, selecting suitable parameters. These powders exhibit high specific areas, up to 250 m^2/g, and original multi-scale morphologies which can be described as spherical substructure (40–3000 nm) composed of individual nanocrystallites (5–30 nm).

Different reaction mechanisms may contribute to powder formation depending on the co-solvent used at the sol stage and on the sol ageing time before starting the supercritical step. These mechanisms strongly influence both the formation of primary crystallites (size and crystalline phase) and the morphology of individual particles. All results presented in this work (powder characteristics, visual observations and phase diagram study) evidenced the competition between two main mechanisms: the condensation reaction and the anti-solvent process. In the case of pentane co-solvent, condensation reaction occurs at the sol stage and is controlled by sol maturation. Then, anti-solvent precipitation is achieved during CO_2 reactor pressurization. With 2-propanol co-solvent, species condensation and anti-solvent precipitation occur simultaneously in CO_2/co-solvent medium and the process kinetics are more hardly controlled. Other co-solvents are currently under study in order to relate the characteristics of the co-solvent/CO_2 mixture, e.g. polarity and dielectric constant, with the 3Y-TPZ powder characteristics.

In other respects, the way in which the SC-CO_2 phase is formed in presence of the sol (in the batch reactor) generates fluctuations in both the CO_2/solvent ratio and reaction kinetics, thus limiting the reproducibility of powder characteristics. In order to solve this problem, an injection device is under study which is able to contact directly the sol with the supercritical CO_2 phase after it has been formed in the reactor.

Acknowledgements

Authors warmly thank the IEM technical staff and particularly Didier COT for FESEM observations, and Abdeslam El MANSOURI for N_2 adsorption–desorption measurements. They also thank the LMAC team of CEA-Pierrelatte for XRD experiments.

References

1. Matson DW, Petersen RC, Smith RD. Formation of silica powder from rapid expansion of supercritical solution. *Advanced Ceramic Materials* 1986;**1**(3):242–6.
2. Matson DW, Fulton JL, Petersen RC, Smith RD. Rapid expansion of supercritical fluid solutions: solute formation of powders, thin films, and fibers. *Industrial and Engineering Chemistry Research* 1987;**26**:2298–306.
3. Chhor K, Bocquet J, Pommier C. Syntheses of submicron TiO_2 powders in vapor, liquid and supercritical phases, a comparative study. *Materials Chemistry and Physics* 1992;**32**:249–54.
4. Chhor K, Bocquet J, Pommier C. Materials science communication—syntheses of submicron magnesium oxide powders. *Materials Chemistry and Physics* 1995;**40**(1):63–8.
5. Pommier C, Chhor K, Bocquet J, Barj M. Reactions in supercritical fluids, a new route for oxide ceramic powder elaboration, synthesis of spinel $MgAl_2O_4$. *Materials Research Bulletin* 1990;**25**:213–21.
6. Pommier C, Chhor K, Bocquet J. The use of supercritical fluids an reaction medium for ceramic powder synthesis. *Silicates Industriels* 1994;**59**(3–4):141–3.
7. Hertz A, Sarrade S, Guizard C, Julbe A. Synthesis and encapsulation of yttria stabilized zirconia particles in supercritical carbon dioxide. *Journal of European Ceramic Society* 2006;**26**(7):1195–203.
8. Guizard C, Julbe A, Sarrade S, Robbe O, Papet S. Chemical reaction of metal-organic precursors in supercritical CO_2. Application to ceramic oxides preparation. In: *Proceeding of the 8th meeting on supercritical fluids: chemical reactivity and material processing in supercritical fluids*. Bordeaux, France: International Society for Advancement of Supercritical Fluids, ISASF; 2002., ISBN 2-905-267-34-8.
9. Guizard C, Julbe A, Robbe O, Sarrade S. Synthesis and oxygen transport characteristics of dense and porous cerium/gadolinium oxide materials: Interest in membrane reactors. *Catalysis Today* 2005;**104**(2–4):120–5.
10. Loy DA, Russick EM, Yamanaka SA, Baugher BM. Direct formation of aerogels by sol–gel polymerizations of alkoxysilanes in supercritical carbon dioxide. *Chemistry of Materials* 1997;**9**:2264–8.
11. Alonso E, Montequi I, Lucas S, Cocero MJ. Synthesis of titanium oxide particles in supercritical CO_2: effect of operational variables in the characteristics of the final product. *Journal of Supercritical Fluids* 2007;**39**(3):453–61.
12. Sarrade S, Schrive L, Guizard C, Julbe A. Manufacture of single or mixed metal oxides or silicon oxide. *PCT Int*., 1998, WO9851613, France.
13. Boulc'h F, Dessemond L, Djurado E. Delay to tetragonal-to-monoclinic transition in water vapour due to nanostructural effect. *Journal of European Ceramic Society* 2004;**24**:1181–5.
14. Basu B, Vleugels J, Biest OVD. Transformation behaviour of tetragonal zirconia: role of dopant content and distribution. *Materials Science and Engineering A* 2004;**366**:338–47.
15. Kiran E, Pöhler H, Xiong Y. Volumetric properties of pentane + carbon dioxide at high pressures. *Journal of Chemical Engineering Data* 1996;**41**:158–65.
16. Gurdial GS, Foster NR, Yun SLJ, Tilly KD. Phase behavior of supercritical fluid–entrainer systems. In: Kiran E, Brennecke JF, editors. *Proceedings of supercritical fluid engineering sciences—fundamentals and applications, ACS symposium series 514*. Washington, DC: American Chemical Society; 1993. p. 34.
17. Polishuk I, Segura JWH. Simultaneous prediction of the critical and sub-critical phase behavior in mixtures using equations of state. II. Carbon dioxide-heavy n-alkanes. *Chemical Engineering Science* 2003;**58**:2529–50.
18. Ziegler JW, Chester TL, Innis DP, Page SH, Dorsey JG. Supercritical fluid flow injection method for mapping liquid–vapor critical loci of binary mixtures containing CO_2. In: *Innovations in Supercritical Fluids.* 73rd ed. Washington, DC: American Chemical Society; 1995. p. 93.
19. Radosz M. Vapor–liquid equilibrium for 2-propanol and carbon dioxide. *Journal of Chemical Engineering Data* 1986;**31**:43–5.
20. Martin A, Cocero MJ. Micronization processes with supercritical fluids: fundamentals and mechanisms. *Advanced Drug Delivery Review* 2008;**60**:339–50.